International Journal of Fluid Machinery and Systems
Vol. 4, No. 3, July-September 2011

DOI: 10.5293/IJFMS.2011.4.3.334
ISSN (Online): 1882-9554

Original Paper

Counter-Rotating Type Pumping Unit (Impeller Speeds in Smart Control)

Toshiaki Kanemoto[1], Keiichi Komaki[2], Masaaki Katayama[3] and Makoto Fujimura[3]

[1] Faculty of Engineering, Kyushu Institute of Technology
[3] Graduate School of Engineering, Kyushu Institute of Technology
Sensui 1-1, Tobata, Kitakyushu 804-8550, Japan
[2] Design Department, Honda Kiko Co., Ltd.
Yamano 2055, Kama 820-0202, Japan

Abstract

Turbo-pumps have weak points, such as the pumping operation is unstable on the positive slope of the head curve and/or the cavitation occurs at the low suction head. To improve simultaneously both weak points, the first author invented the unique pumping unit composed of the tandem impellers and the peculiar motor with the double rotational armatures. The front and the rear impellers are driven by the inner and the outer armatures of the motor, respectively. Both impeller speeds are automatically and smartly adjusted in response to the pumping discharge, while the rotational torques between both impellers/armatures are counter-balanced. Such speeds contribute to suppress successfully not only the unstable operation at the low discharge but also the cavitation at the high discharge, as verified with the axial flow type pumping unit in the previous paper.

Continuously, this paper investigates experimentally the effects of the tandem impeller profiles on the pump performances and the rotational speeds against the discharge, using the impellers whose loads are low and/or high at the normal discharge. The worthy remarks are that (a) the unstable operation is suppressed as expected and the shut off power is scarcely large in the smart control, (b) the blade profile contributes to determine the discharge giving the maximum/minimum rotational speed where the reverse flow may incipiently appears at the front impeller inlet, (c) the tandem impeller profiles scarcely affect the rotational speeds, while the loads of the front and the rear impellers are same, but (d) the impeller with the low load must run faster and the impeller with the high load must run slower at the same discharge to take the same rotational torque, and (e) the reverse flow at the inlet and the swirling velocity component at the outlet of the front impeller with the high load require making the rotational speed of the rear impeller with low load fairly faster at the lower discharge.

Keywords: counter-rotation, tandem impellers, pump, armature, smart control, performance, rotational speed

1. Introduction

The operation of the turbo-pump may be unstable on the positive slope of the head curve, and/or the cavitation may occur in the impeller while the suction head is intolerably low. To improve these unacceptable weak points, the phenomena and the causes have been energetically investigated (Gopalakrishnan et al. [1]), and how to cope with such points have also been proposed for the individual cases. That is, for instance, the unstable operation can be suppressed well with the traditional type swirl-stop, the annular wing (Kaneko et al. [2]), or the additional jet flow along the suction cover just in front of the impeller inlet (Goto [3]). Besides, the inducer is most effective, as well known, to protect the main impeller blade from the cavitation erosion. Both unacceptable weaknesses pointed out above, however, have been investigated and improved individually because they are induced from the essentially different causes in general.

The first author invented the unique pumping unit which can improve simultaneously the weak points mentioned above. The peculiar AC induction motor, with the double rotational armatures in place of the traditional mechanism, was prepared for the unit. The inner and the outer armatures drive the front and the rear impellers, respectively, while the relative rotational speed between both armatures is kept constant and the rotational torque is counter-balanced between both impellers/armatures. These two operating conditions play very important parts to suppress successfully the unstable operation and the cavitation. That is, the rotational speeds of the front and the rear impellers are automatically adjusted pretty well in response to the pumping discharge, so as to make the angular momentum change of the flow through the front impeller coincide with that through the rear impeller. Such operations were named "**smart control**" 8 years ago by the first author and have verified experimentally using the model

Received June 7 2010; accepted for publication May 26 2011: Review conducted by Prof. Seung Jin Song. (Paper number O10013K)
Corresponding author: Toshiaki Kanemoto, Professor, turbo@tobata.isc.kyutech.ac.jp

unit with the axial flow type impellers (Kanemoto et al. [4][5]). The counter-rotating impellers driven separately by the isolated motors have been presented by Prof. Shigemitsu et al. [6][7], but the proposed impellers quite differ from them as the impellers are driven, in the smart control, by the peculiar motor with the double rotational armatures.

This paper investigates experimentally the effects of the impeller profiles not only the pump performances but also on the rotational speeds of the front and the rear impellers against the discharge, using the four kinds of the impellers whose loads are low and/or high at the normal discharge.

2. Counter-Rotating Type Pumping Unit

2.1 Impeller Speeds Predicted in Smart Control

The model pumping unit is shown in Fig. 1. The inner and the outer armatures of the motor are connected directly to the front and the rear impellers, respectively. To understand clearly the discussions in the experimental results, the counter-rotations in the smart control (Kanemoto et al. [4][5]) is briefly reinterpreted. The inner and the outer armatures of the AC induction motor work at the conditions that the rotational torques are counter-balanced and the relative rotational speed between both armatures is kept constant, which is specified with the number of the poles and the frequency supplied from the power grid system. Then, the angular momentum change of the flow through the front impeller must be the same as that through the rear impeller. Assuming the ideal flow condition and the axial flow at the front impeller [see Fig. 2: u, v and w are the rotational velocity (impeller speed), the absolute and the relative velocities, α and β are the absolute and the relative flow angles, the subscripts 1~4 denote the impeller inlet and/or outlet], the flow must run in the axial direction at the rear impeller outlet (α_4=0) regardless of the discharge. The rear impeller speed must decrease at the smaller discharge (the dashed line in Fig. 2) than the normal discharge (the thick solid lines in Fig. 2), to get the axial flow at the outlet. The decrease of the rear impeller speed causes the increase of the front impeller speed, as the relative speed must be kept constant. The increase of the front impeller speed enlarges the attack angle, and brings the reverse flow at the impeller inlet in the actual flow with viscosity, which may make the pumping operation unstable. The reverse flow obstructs the impeller rotation and results in increasing the rotational torque more than the angular momentum change of the flow through the impeller. That is, the reverse flow at the front impeller requires the rear impeller to increase the momentum change by taking the swirling flow component at the outlet (see Fig. 3). Consequently, the front impeller speed comes to decrease in response to the increase of the rear impeller speed in keeping the relative speed constant, and the reverse

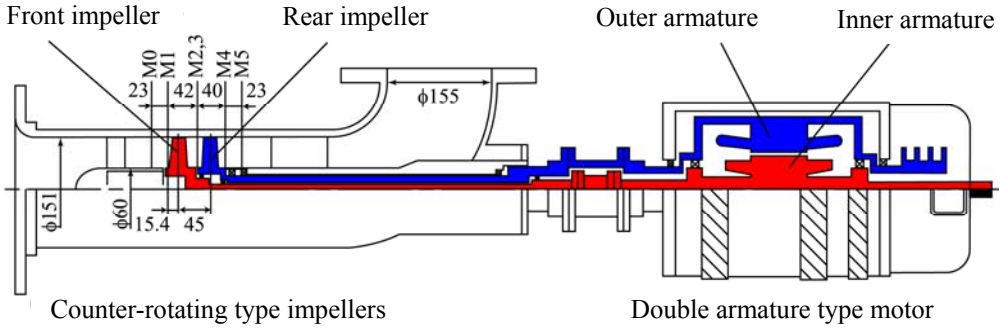

Fig. 1 Model counter-rotating type pumping unit

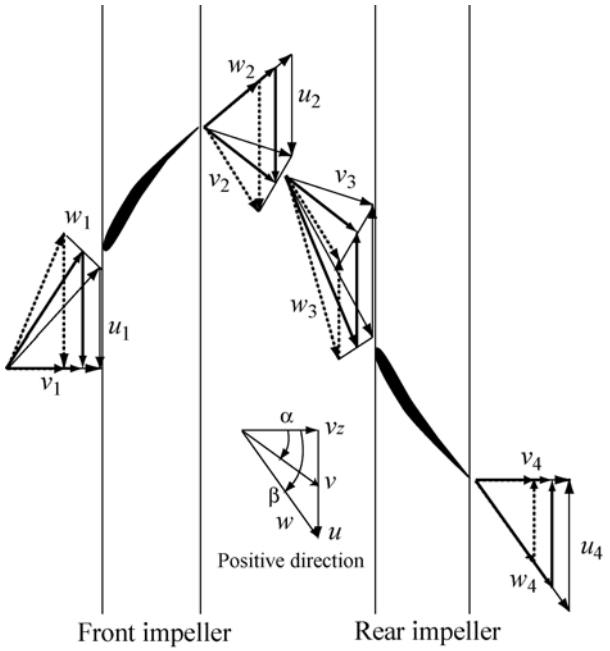

Fig. 2 Velocity triangles at the smart control in the ideal flow

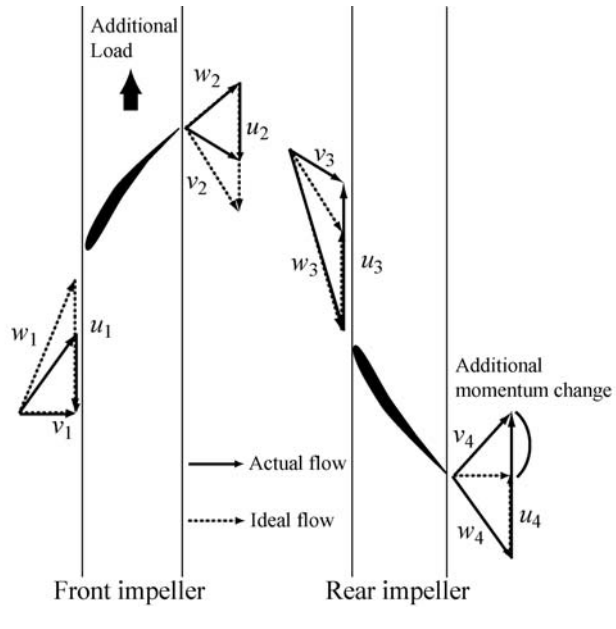

Fig. 3 Velocity triangles at the smart control in the actual flow

Table 1 Inlet and outlet angles of the blade and solidities

Impeller			Blade angle (Deg.)				Solidity	
Front	Rear		β_{d1}	β_{d2}	β_{d3}	β_{d4}	Front	Rear
A	A	Hub	-67.0	0.0	77.9	57.7	0.75	0.75
		Mean	-77.4	-63.0	80.0	69.4	0.75	0.75
		Tip	-80.4	-72.6	81.6	76.4	0.75	0.75
B	B	Hub	-76.9	-14.9	71.9	42.9	0.99	0.89
		Mean	-79.2	-58.0	77.2	70.1	0.82	0.82
		Tip	-80.4	-79.0	79.9	75.9	0.81	0.78

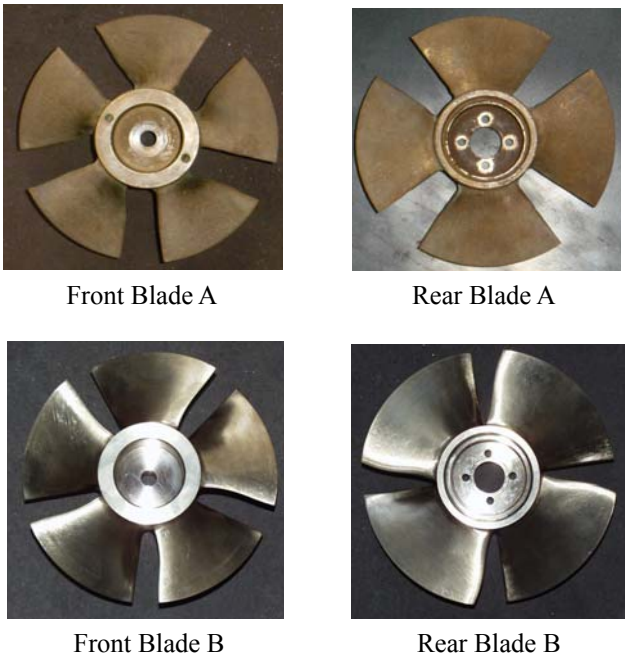

Fig. 4 Front view of the blades

flow is suppressed fruitfully. Then, the pump head lowering in the front impeller is successfully compensated with the head rising in the rear impeller with higher speed. Such rotational speeds suggest that the counter-rotation in the smart control certainly contributes to make the pump operation stable at the low discharge.

At the higher discharge than the normal discharge, the rear impeller has to rotate faster than the front impeller to make the swirl-less flow at the outlet (the thin solid line in Fig. 2). Such rotation suggests that the front impeller works effectively in place of the inducer at the higher discharge.

2.2 Model Impeller Profiles

Euler's head of the counter-rotating type impellers, which are installed in the model pumping unit shown in Fig. 1, is H_{ET} = 4.4 m at the normal discharge Q = 1.78 m^3/min with the impeller speeds n_F = -n_R = 1,500 min^{-1} (subscripts F and R denote the front and the rear impellers, and the positive value is in the rotational direction of the front impeller). The specific speed of the individual impeller is N_S = 1,100 (m, m^3/min, min^{-1}), and the specific speed of the counter-rotating type impellers is N_{ST} = 1,320 (m, m^3/min, min^{-1}). The diameter of both impellers is 150 mm, and the hub ratio is 0.4. The blade numbers of the front and the rear impellers are 5 and 4, respectively. The blade profiles are shown in Table 1 Figs. 4 and 5, where β_d is the inlet or the outlet angles of the blades measured from the axial direction, $R\Theta$ and Z are the distances in the tangential and the axial directions divided by the impeller diameter and measured from the twist centre of the front blade. Front Blade A or B was united respectively with Rear Blade A or B at the design process, then the combination of the front and the rear impellers is called Impeller AA or BB. As for Impeller AA (Kanemoto et al, [5]), the blade thicknesses derived from NACA4409 hydrofoil were distributed along the camber lines of the single arc, the twist centres were placed on the middle position of the camber lines, and the solidities of the front and the rear impellers are 0.75 regardless of the radial position. The excess angle was taken into the outlet angle of the blades to get reasonably the free vortex type flow at the front impeller outlet and the axial flow at the rear impeller outlet (Ikui [8]). The inlet angles of the front and the rear blades were determined so as to meet the relative flow direction, namely the shock-less condition. Impeller BB was designed with the commercial code CFD (TURBOdesign^{-1}: Advanced Design Technology Ltd., DAWES CODE: Ebara Corporation) to improve the pump efficiency (Oba et al. [9]), where the numbers and the diameters of the blades are the same as those of Impeller AA. The solidities of the front and the rear impellers are larger than those of the Impeller AA, namely 0.89 at the hub, 0.82 at the root mean square radius, 0.78 at the tip, to suppress successfully the flow separation on the blade surfaces and the flow deviation at the outlet. The front and the rear blade thicknesses are 0.8 times as thick as those of Impeller AA to reduce the hydraulic losses, in consideration of the material strength. In the following experiments, the authors have prepared not only Impeller AA and BB but also Impeller AB (Front Blade A and Rear Blade B) and Impeller BA (Front Blade B and Rear Blade A).

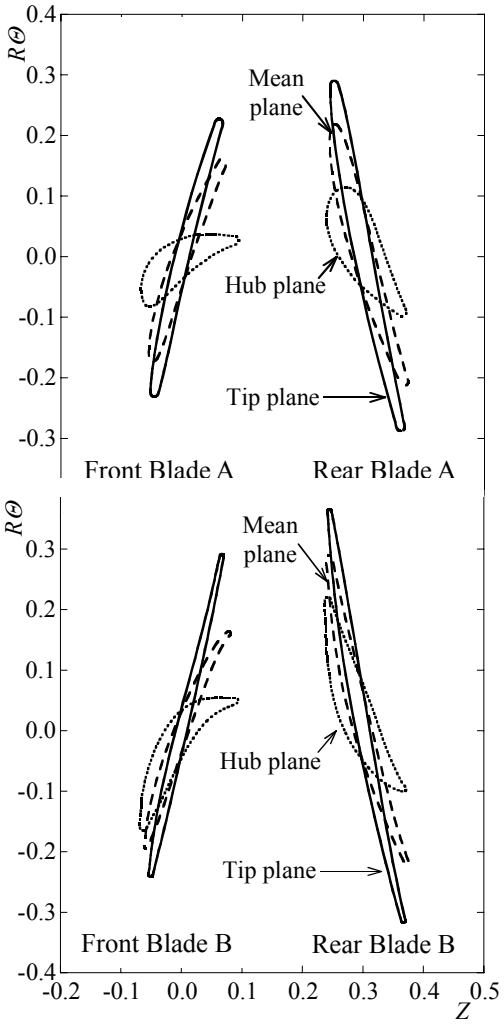

Fig. 5 Cross sections of the blades

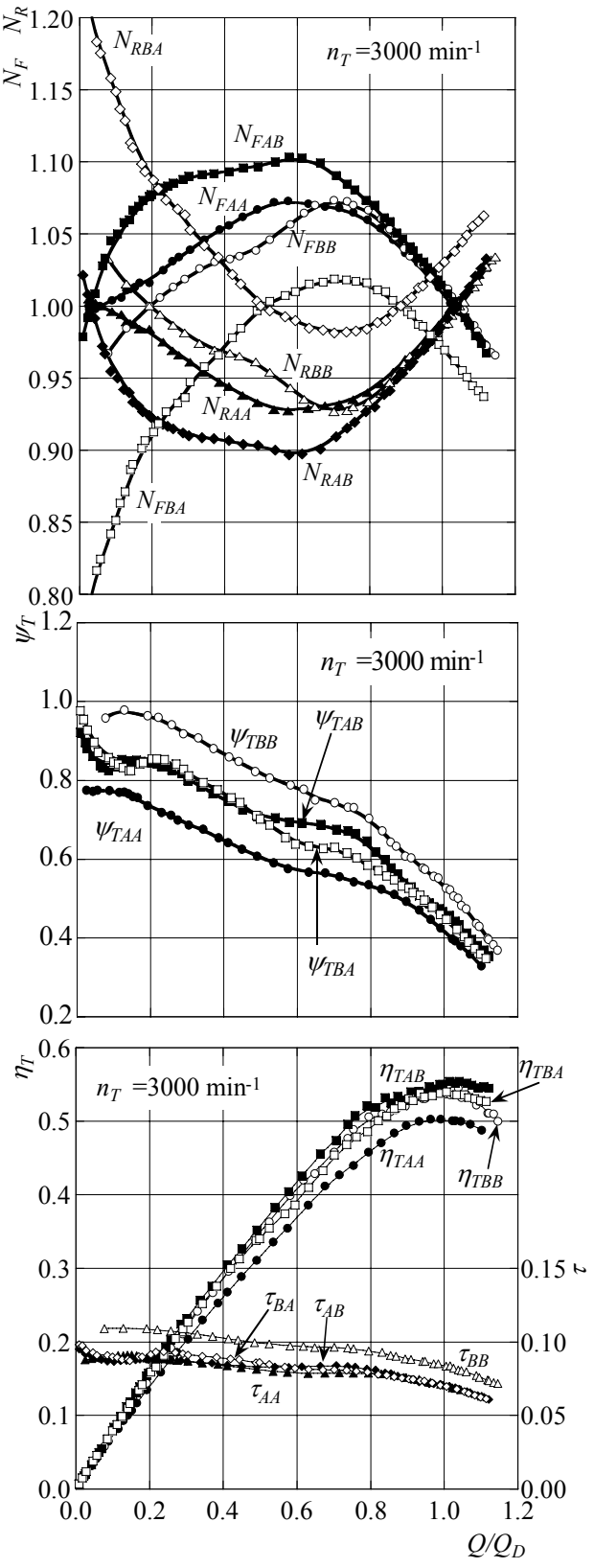

Fig. 6 Pump performance

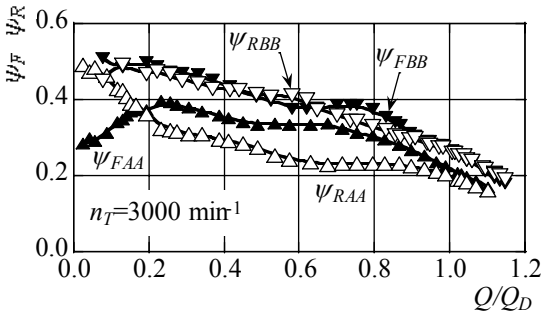

Fig. 7 Heads of the front and the rear impellers

3. Impeller Speeds

3.1 Relation to Pump Performances

Figure 6 shows the pump performances, where the relative rotational speed is kept constant at n_T = 3,000 min^{-1} by means of the inverter control because the rotational speed of the AC induction motors is affected slightly by the torque/discharge. In this figure, Q/Q_D is the discharge ratio (subscript D: the value at the normal operation), ψ_T is the head coefficient [= $H_W/(u_T^2/2g)$, H_W : the pump head estimated from the static pressure on the casing walls at Sections M0 and M5 (see Fig. 1), u_T : the mean rotational velocity (evaluated with the absolute value) at both impeller tips], N is the rotational/impeller speeds [= $n/(n_T/2)$, n : the individual impeller speed (evaluated with the absolute value), the first subscript F and R : value of the front and the rear impellers], τ is the input coefficient [= $P_I/(\rho A u_T^3)$, P_I : the input to the motor], η_T is the total efficiency of the pumping unit [= $\rho g Q H_W/P_I$], and the last two subscripts AA, BB, AB and BA denote the values of Impellers AA, BB, AB and BA, respectively. Impellers AA and BB have the similar rotational speeds against the discharge but the speeds differ obviously from those of Impeller AB and BA. The rotational speed distributions against the discharge of Impeller AB are similar to that of Impeller AA, but the difference between the front and the rear impeller speeds (N_{FAB}, N_{RAB}) are larger than the difference between N_{FAA} and N_{RAA} of Impellers AA, at the moderately low discharge. As for Impeller BA, the rear impeller speed N_{RBA} increases and the front impeller speed N_{FBA} decreases remarkably with the decrease of the discharge.

The shut off powers are scarcely large in the smart control in spite of the axial flow type impellers, and the input coefficients τ_{AA}, τ_{AB}, τ_{BA} take almost the same values though these rotational speeds quite differ as described just above. The input coefficient $\tau_{BB}$of Impeller BB, however, is noticeably larger in comparison with those of Impellers AA, AB and BA. Such results suggest that the momentum change of the flow through the impeller composed of Blade B is larger than that of Blade A, namely Blade B has the higher theoretical head (comparatively high load), due to suppress successfully the flow deviation as expected at the design process (Oba et al. [9]). That is, the impeller composed of Blade A (comparatively low load) must rotate faster than that of Blade B in order to give the same momentum change to the flow through the impeller, in general. The relation between the rotational speeds and the impeller load, momentum change, are also discussed, in detail, in the following sections.

The positive slope causing the unstable operation disappears successfully on the head curves at the moderately low discharge where the positive slope occurs in the traditional axial flow type impeller. The head coefficient ψ_{TBB} of Impellers BB is higher on account of the high theoretical head confirmed just above. The heads ψ_{TAB}, ψ_{TBA} of Impellers AB, BA are almost the same values even if the rotational speeds, N_{FAB}-N_{RAB}, of Impeller AB differ drastically from N_{FBA}-N_{RBA} of Impeller BA. The head ψ_{TAA} of Impeller AA is obviously low and the efficiency η_{TAA} also deteriorates as compared with those of the other impellers. Impeller AA may accompany the larger hydraulic losses than Impeller BB and the rear impeller contributes to increase the losses, as confirmed in Figs. 6 and 7 (ψ_F and ψ_R: the head coefficients of the front and the rear impeller).

3.2 Relation to Rotational Torques

Figure 8 shows the rotational torque T in the smart control at n_T = 3,000 min^{-1}, where the mechanical torque was neglected and the rotational torque of the front impeller is undoubtedly the same as the torque of the rear impeller. The rotational torque T_{BB} of Impeller BB is larger than T_{AA} of Impeller AA irrespective of the discharge, though the rotational speeds of these impellers have nearly the same profiles against the discharge, as shown with N_{FBB}-N_{RBB} and N_{FAA}-N_{RAA} in Fig. 6. It can be reconfirmed that the theoretical head, namely the momentum change, of Impeller BB is larger than one of Impeller AA. Besides, the rotational torques T_{AB}, T_{BA} of Impellers AB, BA are almost the same values close to the mean value between T_{AA} and T_{BB}, though the behaviors of the rotational speeds against the discharge quite differ as shown with N_{FAB}-N_{RAB} and N_{FBA}-N_{RBA} in Fig. 6.

Figure 9 shows the rotational torques of the front and the rear impellers, T_F and T_R in keeping the rotational speed constant (n_F = -n_R = 1500 min^{-1}) regardless of the discharge, where the dashed line is the rotational torque in the smart control given in Fig. 8. The blade profile determines and characterizes not only the rotational torque but also the rotational speeds against the discharge. That is, the rotational torque distribution against the discharge of the front blade T_{FAA} in Impeller AA is almost the same as T_{FAB} in Impeller AB, and T_{FBB} distribution is almost the same as T_{FBA}. Besides, the rotational torque distribution of the rear blade T_{RAA} in Impeller AA is almost the same as T_{RBA} in Impeller BA, and T_{RBB} distribution is almost the same as T_{RAB}. It must be taken into account, however, that the rotational torque of the rear impeller is also affected by the profile and/or the rotational speed of the front impeller. The discharge where T_F = T_R in Fig. 9 meets the discharge where N_F = N_R in Fig. 6, and the lower rotational torque must increase by increasing the rotational speed and the higher torque must decrease by decreasing the rotational speed to take the rotational torque in the smart control shown by the dash line. For instance, T_{FAA} = T_{RAA} at Q/Q_D = 0.15 and 1.01 in Fig 9(a), and then T_{FAA} increases with increasing N_{FAA} and T_{RAA} decreases with decreasing N_{RAA} at Q/Q_D between 0.15 and 1.01. The mean value, however, slightly differs from the torque in the smart control given by the dash line, due to the flow interactions between the front and the rear impellers and the difference of the operating conditions in Figs. 8 and 9.

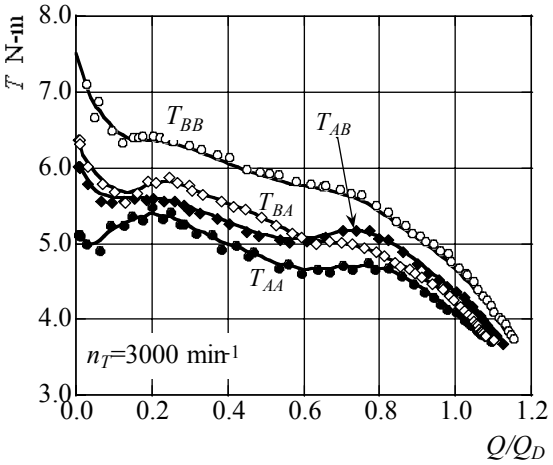

Fig. 8 Rotational torque

3.3 Relation to Flow Conditions

It was verified in the previous papers (Kanemoto et al. [4][5], Oba et

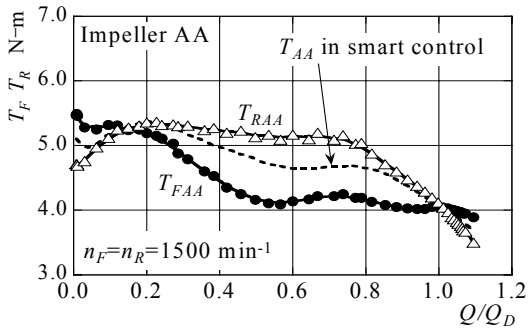

(a) Impeller AA

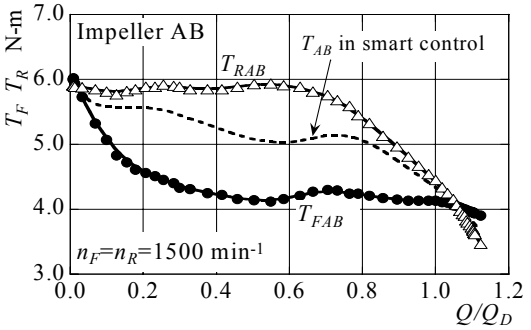

(c) Impeller AB

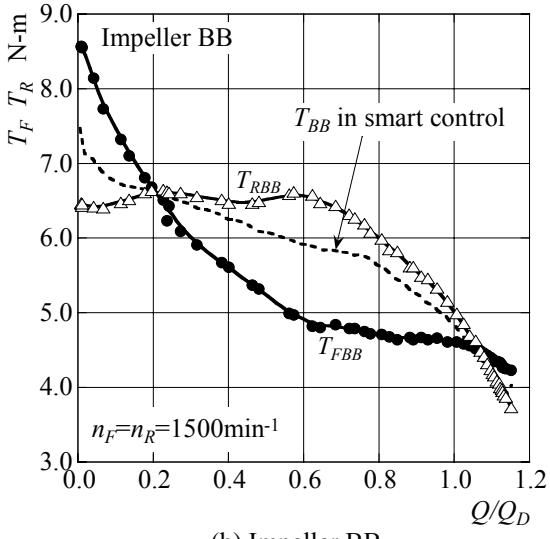

(b) Impeller BB

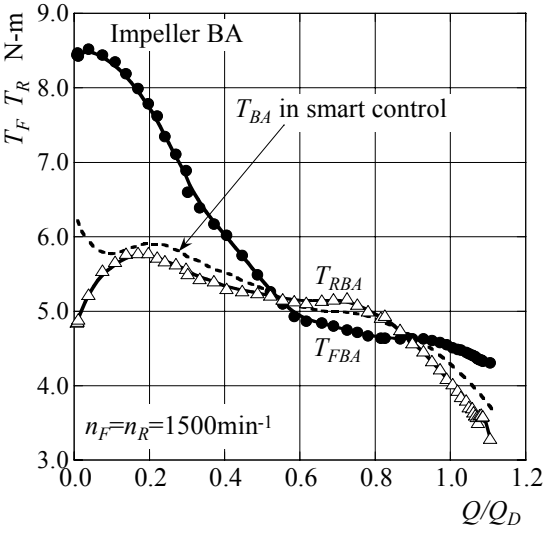

(d) Impeller BA

Fig. 9 Rotational torques in keeping the front and the rear impeller speeds constant

al. [9]) that the flow discharged from the rear impeller has no swirling component while the flow has no swirling component at the front impeller inlet through the fruitful adjustments of the rotational speed in the smart control. Figures 6 and 8 verify that the characteristics described just above, namely the angular momentum change of the flow through the front impeller coincides with that through the rear impeller, do not depend on the blade profiles. The blade profile contributes to determine the discharge giving the maximum/minimum rotational speeds of the front /rear impeller, where the reverse flow may incipiently appears at the front impeller inlet. That is, as confirmed in Fig. 6, the rotational speed N_{FAA} and N_{FAB} of Impellers AA and AB composed of Front Blade A are maximum at Q/Q_D = 0.6, N_{FBB} and N_{FBA} are maximum at Q/Q_D = 0.7, and then the reverse flow makes the front impeller decelerate with the decrease of the discharge.

Figure 10 shows the flow conditions around the front impeller at Q/Q_D = 0.56, where V_M and V_U (positive in the rotational direction of the front impeller) are the meridian and the swirling velocity components divided by u_T giving the mean rotational velocity (absolute) at both impeller tips, Y is the dimensionless distance measured from the hub to the casing walls, and M1, M2/3 are the inlet and the outlet sections located in Fig. 1. Front Blade B causes the reverse flow with the swirling velocity component V_U faster than V_U of Front Blade A, and this angular moment requires the impeller shaft to increase the rotational torque. Resultantly, the rear impeller speed N_{RBB} of Impeller BB must increases to make the angular momentum change large, and then the front impeller speed N_{FBB} comes to be slower than N_{FAA} of Impeller AA. The momentum change through the impeller composed of Front/Rear Blade B is also larger than that of Front/Rear Blade A owing to suppress the flow deviation at the outlet, as discussed above. As for Impeller BB, the higher swirling velocity component at the front impeller outlet and the small inlet angle of the rear blade (β_{d3} in Table 1) make the attack angle to Rear Blade B large in comparison with that to Rear Blade A, even at the normal discharge as shown in Fig. 11. Such unacceptable inlet flow, which is conspicuous with the decrease of the discharge, cannot give enough the momentum change because of the flow separation on the suction surface of Rear Blade B whose thickness is thin. Resultantly, the rotational speed of the rear impeller must increase and then the speed of the front impeller must decreases, which may promote the difference of the rotational speeds between Impellers AA and BB at the same discharge.

The difference of the rotational speed between Front Blade A and Rear Blade B, in Impeller AB, is larger than that of Impellers AA and BB. The reverse flow derived from the impeller composed of Front Blade A does not affect strongly the

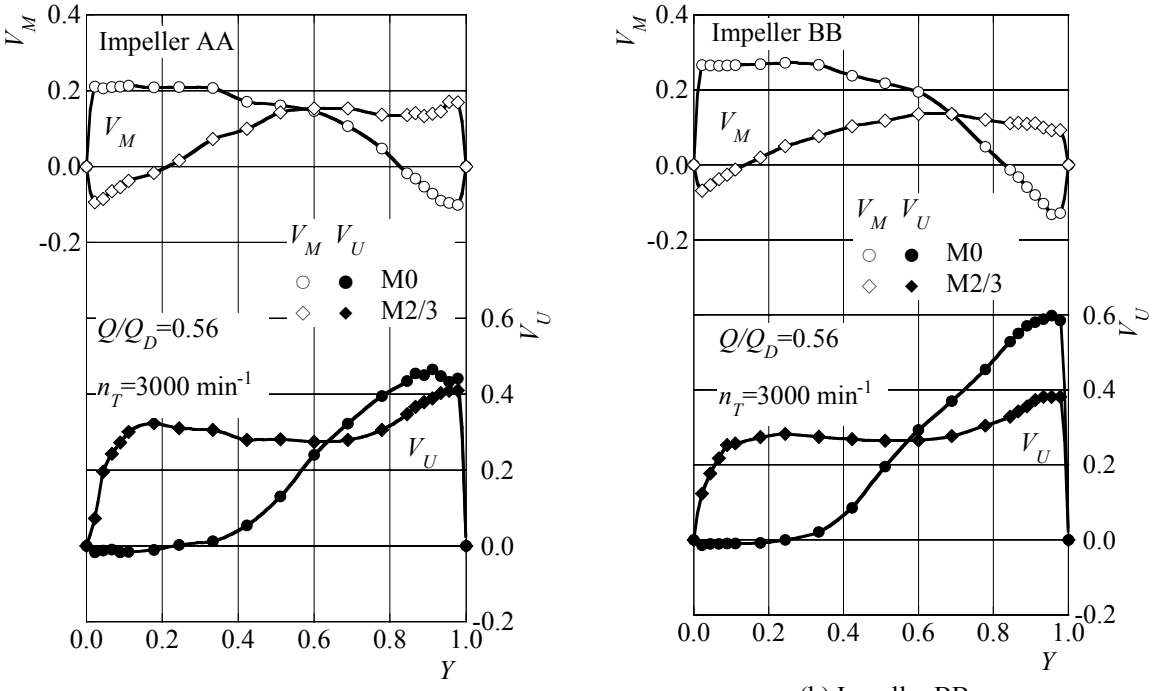

(a) Impeller AA (b) Impeller BB

Fig. 10 Flow conditions around the front impeller at Q/Q_D = 0.56

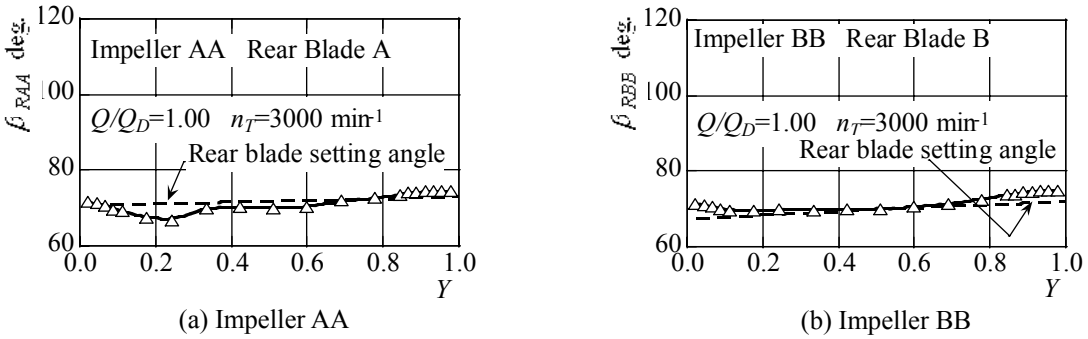

(a) Impeller AA (b) Impeller BB

Fig. 11 Relative flow angle at the rear impeller inlet (Q/Q_D = 1.0)

rotational torque and the swirling velocity component is slow at the front impeller outlet, because of the comparatively lower blade load. That is, the attack angle at the inlet and the flow deviation at the outlet of Rear Blade B are small, and the rear impeller must not increase the rotational speed even at the moderately lower discharge.

The front impeller speed of Impeller BA meets the rear impeller speed at not only the higher but also the lower discharge than that of Impellers AA, BB, AB. The angular moment induced from the reverse flow from Front Blade B is remarkably large with the decrease of the discharge, as presumed above. Besides, the rear impeller composed of Rear Blade A cannot give enough the angular momentum change to the through-flow at the ordinarily rotational speed, as the flow along the suction surface of Rear Blade A may separate with the large attack angle derived from the Front Blade B. Such abnormal flow conditions require making the rotational speed of Rear Blade A fairly faster than that of the other impeller at the lower discharge.

4. Concluding Remarks

The effects of the tandem impeller profiles, which are installed in the counter-rotating type pumping unit, not only on the pump performances but also on the rotational speeds were investigated experimentally, using four kinds of the axial flow type tandem impellers whose loads are low and/or high at the normal discharge. The pump performances and both impeller speeds are affected by not only the discharge but also the impeller profiles. This paper discussed the impeller speeds relation to the pump performances, the rotational torques and the flow conditions around the impeller. The concluding remarks are as follows.

(1) The unstable operation is suppressed as expected at the design process and the shut off power is scarcely large in the smart control regardless of the impeller profiles, while the rotational torque of the front impeller meets undoubtedly and automatically the torque of the rear impeller.

(2) The blade profile contributes to determine the discharge giving the maximum/minimum rotational speeds of the front/rear impellers, where the reverse flow may incipiently appears at the front impeller inlet, and then the rotational speed are affected by the reverse flow at the lower discharge.

(3) The tandem impeller profiles scarcely affect the rotational speeds, while the load of the front impeller is almost the same as one of the rear impeller at the normal operation. The impeller with the low load, however, must run faster and the impeller with the high load must run slower at the same discharge, in order to take the same rotational torque.

(4) The reverse flow at the inlet and the swirling velocity component at the outlet of the front impeller with the high load require making the rotational speed of the rear impeller with low load fairly faster at the lower discharge.

Acknowledgments

The authors wish to thank Dr. Shin Oba and Mr. Shintaro Ito, graduated from Kyusyu Institute of Technology in Japan, for the design of the Impellers and helping some parts of the experiments.

References

[1] Gopalakrishnan, S., Hergt, P. H., Ohashi, H. and Tsujimoto, Y., 1999, “Pump Research and Development: Past, Present and Future,” ASME, Journal of Fluid Engineering, Vol. 121, pp. 237-258.

[2] Kaneko., K. et al, 1990, “Passive Control of Unstable Characteristics of a High Specific Speed Diagonal-Flow Fan by an Annular Wing,” ASME Paper 90-GT-159, 1-7.

[3] Goto, A., 1994, “Suppression of Mixed-Flow Pump Instability and Surge by the Active Alternation of Impeller Secondary Flow,” Transactions of ASME, Journal of Turbomachinery, Vol. 116, pp. 621-628.

[4] Kanemoto, T. and Oba, S., 2002, “Proposition of Unique Pumping System with Counter-Rotating Mechanism,” Proceedings of the 9th International Symposium on Transport Phenomena and Dynamics of Rotating Machinery, FD-ABS-031, pp.1-8.

[5] Kanemoto, T., Kimura, S., Oba, S. and Satoh, M., 2002, “Smart Control of Axial Flow Pump Performance by Means of Counter-Rotation (Counter-Rotating Type and Performance),” JSME International Journal, Series B, Vol. 45, No. 2, pp.293-300.

[6] Shigemitsu, T., Fukutomi, J. and Okabe, Y., 2010, “Performance and Flow Condition of Small-Sized Axial Fan and Adoption of Contra-Rotating Rotors,” Journal of Thermal Science, Vol. 19, No. 1, pp.1-6.

[7] Shigemitsu, T., Furukawa, A., Watanabe, S. and Okuma, K., 2009, “Internal Flow Measurement with LDV at Design Point of Contra-Rotating Axial Flow Pump,” Journal of Fluid Science and Technology, Vol. 4, No.3, pp.723-734.

[8] Ikui, T. 1970, “Blowers and Compressors,” p. 239, Asakura Publishing Co., Ltd. , in Japanese.

[9] Oba, S. and Kanemoto, T., 2004, “Design of Counter-Rotating Impellers by Inverse Method to Improve Pump Performances,” Proceedings of the 22th IAHR Symposium on Hydraulic Machinery and Systems, CD-ROM B9-1.